NOTATION

$c'\rho'$, volume heat capacity of tungsten; c_p, ρ, λ, heat capacity, density, and thermal conductivity of gas studied; l, mean free path length; r, filament radius; α, thermal accommodation coefficient of atoms on tungsten; $\gamma = 1.7811$; ξ, radiation correction; U, voltage across filament; R, filament resistance; L, filament length; E_3, amplitude of third-harmonic voltage; x_2, molar fraction of diatomic molecules in vapor; T, temperature.

LITERATURE CITED

1. C. Lee and C. F. Bonilla, in: Proceedings of the Seventh Conference on Thermal Conductivity, National Bureau of Standards, Maryland (1967).
2. N. B. Vargaftik and V. V. Kerzhentsev, Teplofiz. Vys. Temp., 10, No. 1 (1972).
3. D. L. Timrot, V. V. Makhrov, V. I. Sviridenko, and B. F. Reutov, Teplofiz. Vys. Temp., 14, No. 5 (1976).
4. L. I. Zarkova and B. I. Stefanov, Teplofiz. Vys. Temp., 14, No. 2 (1976).
5. G. I. Gushchin, V. A. Subbotin, and É. Kh. Khachaturov, Teplofiz. Vys. Temp., 13, No. 4 (1975).
6. B. I. Stefanov, L. I. Zarkova, and D. Oliver, Teplofiz. Vys. Temp., 14, No. 1 (1976).
7. N. B. Vargaftik, Yu. K. Vinogradov, and N. A. Vanicheva, Sb. Tr. Mosk. Aviats. Inst., No. 319, 59 (1975).
8. N. B. Vargaftik, Yu. K. Vinogradov, and I. A. Khludnevskii, Thermophysical Properties of Gases [in Russian], Nauka, Moscow (1973).
9. É. Ya. Zandberg and N. I. Ionov, Surface Ionization [in Russian], Nauka, Moscow (1969).
10. N. N. Stolovich and N. S. Minitskaya, Temperature Dependences of Thermophysical Properties of Certain Metals [in Russian], Nauka i Tekhnika, Minsk (1975).
11. A. Kröner, Ann. Phys., 40(4), 438 (1913).
12. M. L. Hackspill, Ann. Chem. Phys., 28(8), 613 (1913).
13. J. O. Hirschfelder, C. F. Curtiss, and R. B. Bird, Molecular Theory of Gases and Liquids, Wiley (1964).
14. J. O. Hirschfelder, J. Chem. Phys., 26, 274 (1957).
15. V. S. Yargin, Sb. Tr. Mosk. Aviats. Inst., No. 319, 75-90 (1975).
16. D. L. Timrot, V. V. Makhrov, and V. I. Sviridenko, Teplofiz. Vys. Temp., 14, No. 1 (1976).

DETERMINATION OF THE THERMAL AND ELECTRICAL CONDUCTIVITIES OF ULTRAFINE PARTICULATE SYSTEMS

G. N. Dul'nev, Yu. P. Zarichnyak, and V. V. Novikov

UDC 536.24:537.321

An ultrafine particulate system with a linear particle deformation close to zero is investigated. The thermal and electrical conductivities are determined with regard for dimensional effects at the contacts.

The figure of merit of thermoelectric materials is governed by the Ioffe parameter $z = \alpha^2\sigma/\lambda$ [1], which implies that in order to increase the thermoelectric figure of merit at constant α it is necessary to increase the ratio $\beta = \sigma/\lambda$ [1, 2].

There has been recent discussion in the literature of the possibility of increasing the thermoelectric figure of merit of a material on the basis of an ultrafine dispersed system with average linear grain size from 100 to 2000 Å, which has been subjected to superficial sintering. Experimental studies of such a system [3] have shown that the value of z is increased severalfold over the value z_1 for the monolithic material.

An experimental study of σ, α, and λ has been carried out [6] for a high-porosity ($m_2 \approx 0.7$) particulate system with a mean grain size $d \sim 2$ μm obtained from n-Ge. The ratio $\beta = \sigma/\lambda$

Leningrad Institute of Precision Mechanics and Optics.

Translated from Inzhenerno-Fizicheskii Zhurnal, Vol. 34, No. 5, pp. 860-869, May, 1978. Original article submitted February 1, 1977.

0022-0841/78/3405-0588$07.50

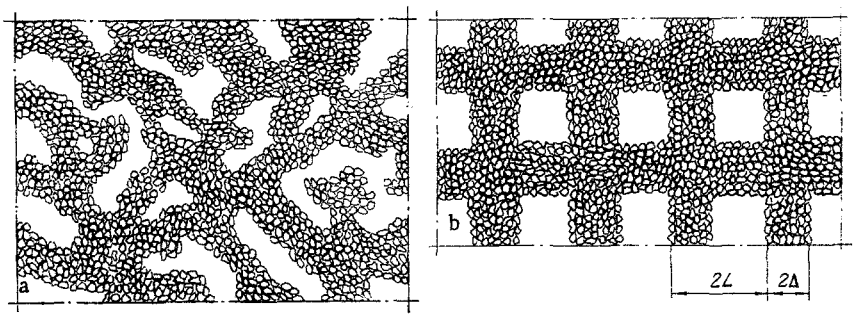

Fig. 1. Structure and model of the ultrafine system. a) Actual structure; b) model of ultrafine system.

for four samples was varied from 10 to 400, and $z = (3\text{-}6)z_1$, confirming the conclusions of [3].

In all the investigations except [5] the experimental results are interpreted by qualitative analysis of heat-transfer and electrical charge transfer processes. The authors of [5] have attempted to explain the experimental results on the basis of the models and equations of Odelevskii [7], Dul'nev [8], and Vasil'ev [9], which are widely used in determining the values of λ for porous materials. This approach, however, ignores contact dimensional effects, which affect the transfer processes in such systems and thus yield an unsatisfactory description of the experimental data.

Below we propose a model and equations for determining the effective thermal and electrical conductivities λ and σ of an ultrafine-grained system for which the linear particle deformation is close to zero, with regard for dimensional effect at the contacts.

Model of the Particulate System

In particulate systems having a porosity $m_2 > 0.4$ we distinguish a first-order structure, or "matrix," which consists of a relatively dense bed of grains in constant contact, and a second-order structure comprising a three-dimensional lattice of larger voids permeating the matrix [10] (Fig. 1). Consequently, the determination of the thermal and electrical conductivities of the particulate system is divided into two stages. First the conductivity Λ_m of the matrix is determined, and then on the basis of the Frei—Dul'nev model with interpermeating components the effective conductivity Λ of the particulate system is determined according to the expression [11]

$$\Lambda = \Lambda_m\left[\frac{C^2 - \nu(1-C)C}{\nu C(1-C) + (1 - C + C^2)} + \nu\,\frac{C(1-C) + \nu(1-C)^2}{C(1-C) + \nu(1 - C + C^2)}\right], \tag{1}$$

in which $\nu = \Lambda_2/\Lambda_m$ and $C = \Delta/L$ is determined from the equation

$$2C^3 - 3C^2 + 1 = m_{22}. \tag{2}$$

Here m_{22} is the porosity of the second-order structure (Fig. 2) [10]:

$$m_{22} = (m_2 - m_{2m})/(1 - m_{2m}), \tag{3}$$

where m_{2m} is the porosity of the matrix. The conductivity Λ_m, which represents the thermal or electrical conductivity of the matrix, is determined on the basis of the average unit element of a particulate system with a totally disordered structure (Fig. 2) [10]. The geometrical dimensions of the average element are determined from the expressions

$$y_3 = 2\sqrt{N_m - 1}/N_m;\quad y_4 = y_3/\sqrt{1 - m_{2m}^0}; \tag{4}$$

$$\bar{h}_1 = 1 - \varkappa_m - \sqrt{1 - y_3^2};\quad N_m = (m_{2m}^0 + 3 + \sqrt{(m_{2m}^0)^2 - 10\,m_{2m}^0 + 9})/2m_{2m}^0, \tag{5}$$

in which $y_i = r_i/r$, $\bar{h}_1 = h_1/r$, and $\varkappa_m$ is the linear shrinkage of the average element due to pressing and sintering of the particulate system. For particulate systems in the free-flowing state with elastic deformation of the particles $\varkappa_m$ can be taken equal to zero.

Particulate Systems with $\varkappa_m \simeq 0$

Particulate systems of this type include systems in the free-flowing state under a specific pressure not greater than 10 kg/cm², i.e., systems in which the particles are subjected

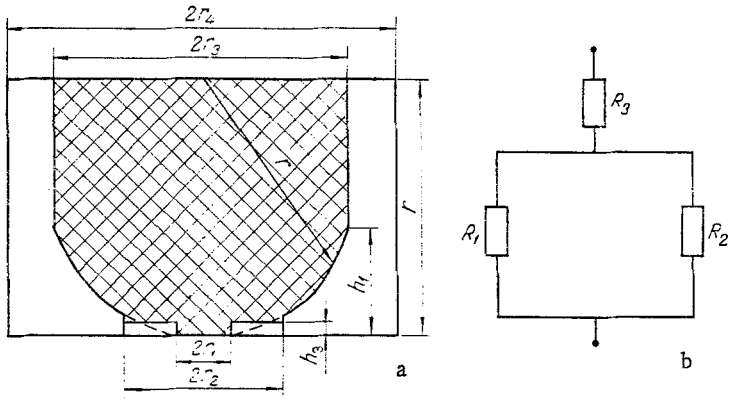

Fig. 2. Diagram to determine the thermal and electrical conductivity of the matrix: a) averaged element of a disordered structure of the matrix; b) equivalent wiring scheme of electrical resistances.

only to elastic deformations. The radius of the nominal contact spot between spherical particles in this case is determined according to the classical Hertz theory [12] from the expression

$$y_2 = \sqrt{\frac{3}{4}\pi y_4^2 P'_{sp}/E_S}, \tag{6}$$

in which E_S is the elastic modulus of the particulate system, $P'_{sp} = P_{sp} + G$, P_{sp} is the specific external pressure, $G = 1.6\rho_1 m_1 h_{\mathcal{L}\alpha}/y_4^2$ is the specific force of gravity of the higher layers, and $h_{\mathcal{L}\alpha}$ is the height of the layer of particles.

The nominal contact area of real coarse particles is greater, because the elastic modulus of the rough layer (consisting of microasperities and the gas spaces between them) is less than the elastic modulus of the particle material itself. The modulus E_S and the elastic modulus of the particle material E_M are related as follows [13]:

$$E_S = k_E (P'_{sp})^{1/3} E_M^{2/3}, \tag{7}$$

where K_E is an empirical coefficient, which varies between 0.5 and 1 for various materials.

Experimental studies [13] have shown that E_S for various materials (glass and steel balls, lead shot, quartz sand) at $P_{sp} < 3$ kg/cm^2 is practically constant and equal to $E_S \approx 650$ kg/cm^2. We can therefore rewrite (6) on the basis of (7) as follows:

for small loads ($P'_{sp} < 3$ kg/cm^2)

$$y_2 = 0.15\, y_4^{2/3} (P'_{sp})^{1/3}, \tag{8}$$

for large loads (3 kg/cm^2 < P'_{sp} < 14 kg/cm^2)

$$y_2 = 1.4\, y_4^{2/3} (P'_{sp}/E_M)^{2/9}. \tag{9}$$

The actual contact area $S_a = \pi r_1^2$ usually constitutes a very small fraction of the nominal area S_n and is related to it [10, 13] by the expression $S_a = \eta_1 S_n$, where η_1 varies in the interval $10^{-2} \geqslant \eta_1 \geqslant 10^{-5}$. Therefore, the relation between y_1 and y_2 can be expressed in the form

$$y_1 = (3.3 \cdot 10^{-3} - 1 \cdot 10^{-1})\, y_2. \tag{10}$$

Annealing of Particulate Systems

Annealing of a particulate system is accompanied by concretion (sintering) of the contacts between particles. Ideal sintering occurs when the contact surfaces are free of extraneous impurities, are atomically smooth, and are arranged in such a way as to establish a one-to-one correspondence in the positions of the atoms of both particles. However, this ideal situation is practically never realized. All real surfaces have a relief (roughness), so that in the first stage of sintering, when plastic crumpling of the irregularities takes place, along with a process of "structural lining up" in the positions of the atoms, in the contact zone there are always micropores, which act as a source or sink of vacancies [14]. The contact spot in sintering can be estimated from the expression [14]

$$y_2 = (At)^n, \tag{11}$$

in which A and n are constants depending on the sintering kinetics and t is the sintering time.

The relation between y_2 and y_1 in the first stage of sintering is analogous to (10).

Before determining the thermal and electrical conductivities of the "matrix" we give a definition of the actual contact spot. Here we interpret the actual contact spot to mean the area of the contacting surfaces wherein "structural lining up" takes place and atomic bonds are formed on the contacting parts. The real surfaces of a crystal always have a relief (roughness), so the regions in which "structural lining up" take place appear as isolated spots wherever there is close correspondence in the positions of the atoms. The formation of atomic bonds on the contacting parts occurs immediately in the first stage of sintering [14].

Consequently, the contact between particles is modeled by an area of actual contact with radius r_1 and a contact-adjacent gap with a height equal to the height h_r of the particle microasperities (roughness height). The relation between the particle microasperity h_r and diameter d for metal particles can be written in the form $h_r = k_M \cdot 10^{-3} d$ [10, 13, 15]. The coefficient k_M varies in the interval from 0.5 to 1 [15].

Electrical Conductivity of the Average Element

In determining the effective electrical conductivity of the average element we make use of the fact that a current flows across the thin layer of the contact gap if the height of the gap is of the order of a few tenths of an angstrom unit, due to the tunnel effect and thermionic emission.

The contact gap has a complex profile, the height of which varies from zero to h_r [10]. The current across the gap can become commensurate with the current across the actual contact spot if the height of the gap $h_e < 100$ Å; see expressions (17)-(19) below. Consequently, the current across the contact gap does not flow over the entire area $S_2 = \pi(r_2^2 - r_1^2)$, but through the area of the gap $S_e = \pi(r_{2e}^2 - r_1^2)$, the height of which is equal to h_e. The relation between r_2 and r_{2e} can be determined from geometrical constructions: $r_{2e} = r_2$; $\varepsilon = h_e/h_r$.

Now the electrical resistance R_c of the contact spot is determined simultaneously with the combined resistance R_1 of the actual contact spot and the resistance R_2 of the contact gap; i.e.,

$$R_c^{-1} = R_1^{-1} + R_2^{-1}, \tag{12}$$

where $R_1 = 0.5\, h_e/\sigma_1 \pi r_1^2$ is the resistance of the actual contact spot and is equal to the resistance of a plane wall of height equal to half the average height h_e, $R_2 = 0.5\, h_e/\sigma_2 \pi(r_{2e}^2 - r_1^2)$ is the resistance of a plane contact gap of height h_e, and σ_1, σ_2 are the electrical conductivities of the particle and contact gap, respectively.

The total electrical resistance of the average element (see Fig. 2) is

$$R_\Sigma = R_c + R_3, \tag{13}$$

where $R_3 = (r - 0.5\, h_e)\Phi/\sigma_1 \pi r_{2e}^2$ is the resistance to the spreading current across the contact, and Φ is the spreading function of the current lines.

Knowing that R_Σ can be written in the form $R_\Sigma = r/\pi r_4^2 \sigma_m$, we determine the effective electrical conductivity of the average element in the form

$$\sigma_m = \sigma_1 \frac{y_{2e}^2}{y_4^2} \cdot \frac{y_1^2 + \nu(y_{2e}^2 - y_1^2)}{0.5 y_{2e}^2 \bar{h}_e + (1 - 0.5\bar{h}_e)\Phi[y_1^2 + \nu_2(y_{2e}^2 - y_1^2)]}, \tag{14}$$

where $\bar{h}_e = h_e/r$ and $\nu_2 = \sigma_2/\sigma_1$.

The analytical form of the function Φ is given in [10] and for $y_{2e} \leqslant 5 \cdot 10^{-2}$ can be approximately written

$$\Phi = 0.017 + 0.4 y_{2e} \tag{15}$$

or for $y_{2e} \geqslant 0.1$ in the form $\Phi \approx y_{2e}$.

It is evident from (12) that conditions can arise such that the area of the actual contact spot plays only a secondary role in the effective electrical conductivity of a particulate

system if that area is relatively small and if the gap between the particle surfaces remains of the order of a few tenths of an angstrom unit at distances much greater than the dimensions of the actual contact spot, i.e., for $y_2 \gg y_1$ if $h_r \ll 10^2$ Å.

Using the fact that $h_r \approx 10^{-3}d$, we infer that these conditions can arise if the mean particle diameter $d \ll 10$ μm and the system is very lightly sintered ($\varkappa_m \approx 0$).

Electrical Conductivity of a Plane Gap

To determine the electrical conductivity of the gap it is necessary to solve two fundamental problems: 1) to determine the conduction mechanism in the gap; 2) to determine the shape of the potential barrier and the geometrical dimensions of the gap.

Electrons can flow across the potential barrier of the gap under the following conditions: The electrons in the conduction band have sufficient thermal energy to overcome the potential barrier of the gap and to penetrate into the conduction band of the other conductor; this mechanism is called thermionic emission; if the potential barrier of the gap is greater than the thermal energy of the electrons, they can penetrate the barrier by the tunneling effect.

Both of these mechanisms are often observed simultaneously, and the question as to which one is predominant is decided by the work function, the width of the gap, and the temperature. The following inequality can be used to estimate which mechanism is predominant [16]:

$$h_e < \frac{\hbar}{2KT}\left(\frac{\bar{v}}{2m^*}\right)^{1/2}. \tag{16}$$

If inequality (16) holds, the tunneling current dominates, and for the opposite inequality thermionic emission is predominant.

Inasmuch as the number of contacts in the direction of current flow is large, the voltage drop across a single contact is small. The thermionic emission conductivity of the gap at small gap voltages is [17]

$$\sigma_{2g} = \frac{CeTh_e}{K}\exp\left(-\frac{\bar{v}}{2KT}\right). \tag{17}$$

The conductivity of a gap between metal electrodes at small voltages in connection with tunneling transition of electrons is [18]

$$\sigma_{2X} = \left(\frac{l}{\hbar}\right)^2 (2m^*\bar{v})^{1/2}\exp\left[-\frac{2h_e}{\hbar}(2m^*\bar{v})^{1/2}\right]. \tag{18}$$

If the electrodes are isotopic semiconductors, then the conductivity of the gap can be expressed in the form

$$\sigma_{2S} = 22.56\,\frac{\varepsilon_2 E_F^{3/2}\bar{v}}{(m^*)^{1/2}\delta(\bar{v}+E_F)}\exp\left[-\frac{2h_e}{\hbar}(2m^*\bar{v})^{1/2}\right], \tag{19}$$

where $\delta = \sqrt{\varepsilon_2(\varphi_0 - eV)/2\pi e^2 n_0}$ is the depth of penetration of the field into the semiconductor.

The expression (19) for σ_{2S} has been derived on the basis of [19].

Here $\bar{v}$ is the height of the gap potential barrier; at point x it is equal to

$$v(x) = \varphi_0 - eEx + \varphi^*, \tag{20}$$

where φ_0 is the electronic work function of the conductor, E is the electric field at the contact, and φ^* is the image force potential, which is equal to [20]

$$\varphi^* = -\frac{e^2}{4\pi\varepsilon_2}\left\{\sum_{n=0}^{\infty}\frac{\varepsilon_{12}^{2n}}{nh_e} + \varepsilon_{12}\sum_{n=0}^{\infty}\frac{\varepsilon_{12}^{n}}{2(nh_e+x)} + \varepsilon_{12}\sum_{n=1}^{\infty}\frac{\varepsilon_{12}^{2(n-1)}}{2(nh_e-x)}\right\}, \tag{21}$$

where $\varepsilon_{12} = (\varepsilon_1 - \varepsilon_2)/(\varepsilon_2 + \varepsilon_1)$ is the reduced dielectric constant.

The height of the potential barrier can be determined by solving the equation [21]

$$\left.\frac{\partial v}{\partial x}\right|_{x=x_0} = 0, \tag{22}$$

in which x_0 is the distance at which the potential energy is a maximum.

If only the first moments of the image forces are included in (22), then on the basis of (21) we obtain for the height of the potential barrier in the gap

$$\bar{v} = \varphi_0 \left\langle 1 - \mu \left\{ \sqrt{1+\eta} - 2\,\frac{\varepsilon_2}{\varepsilon_2+\varepsilon_1} + \frac{1}{2}\,\eta^2 \left[\left(\sqrt{1+\eta} - 1 \right) \sqrt{1+\eta} \right]^{-1} \right\} \right\rangle , \tag{23}$$

where

$$\mu = e^2\varepsilon_{12}/4\pi h_e \varphi_0 \varepsilon_2;\ \eta = 4\pi E \varepsilon_2 h_e / e\varepsilon_{12} .$$

The contact field E can be approximately determined from the expression

$$E = \frac{dV}{h_{la} h_e} , \tag{24}$$

where V is the voltage applied to the sample (in volts).

Expressions (17)-(19), (23), and (24) enable us to determine the electrical conductivity in the contact gap.

Thermal Conductivity

The thermal conductivity λ_m of the average element has been determined in [10] and is equal to

$$\lambda_m = \frac{\lambda_1}{y_4^2} \left\langle \left[\frac{y_1^2}{0.5\bar{h}_r + (1 - 0.5\bar{h}_r)\,\Phi} + \right. \right.$$
$$+ \left\{ \frac{D}{y_3^2} + \left[\frac{(y_2^2 - y_1^2)\,\nu_{M3}}{(1 - 0.5\bar{h}_r - B) + 0.5\bar{h}_r} + \frac{2\nu_g}{1-\nu_g} \times \right. \right.$$
$$\left. \left. \left. \times \left(D - F + w \ln \frac{w - D}{w - F} \right) \right]^{-1} \right\}^{-1} + \nu_{2SP}(y_4^2 - y_3^2) \right\} \Big\rangle . \tag{25}$$

Here the quantities $\nu_g = \lambda_g/\lambda_1$; $\nu_{M3} = \lambda_{M3}/\lambda_1$; $\nu_{2SP} = \lambda_{2SP}/\lambda_1$; $\nu_{S3} = \lambda_{S3}/\lambda_1$; $w = [1 - \nu_{S3}D + B/Hd](1 - \nu_{S3})$ account for molecular and radiative heat conduction in the pores and contact gaps; expressions for them are given below; also, λ_1 is the thermal conductivity of the particles, and $D = \sqrt{1 - y_3^2}$, $F = \sqrt{1 - y_2^2}$.

Radiative and Molecular Thermal Conductivity of the Filler Gas in the Pores

An analysis of the thermal conductivity for radiative and molecular heat transfer in the pores of a particulate system is carried out in [10, 14]. The expressions for λ_i for a plane gas interlayer of thickness h_i between plates are written in the form

$$\lambda_i = \lambda_g [1 + B/(Hh_i)]^{-1} + \varepsilon_{re}\sigma_{S\text{-}B}\, T^3 h_i , \tag{26}$$

where B has the form

$$B = \frac{4\gamma}{1+\gamma} \cdot \frac{2-a}{a}\, \Lambda_0 H_0 \,\mathrm{Pr}^{-1} . \tag{27}$$

Here λ_g is the thermal conductivity of the filler gas, a is the accommodation coefficient of the gas at the walls, $\gamma = c_p/c_v$ is the adiabatic exponent, Pr is the Prandtl number, and Λ_0 is the mean free path of the gas molecules at atmospheric pressure H_0 and temperature T_0. The second term in (26) characterizes the contribution of radiative energy transfer to the thermal conductivity.

The expressions for the coefficients λ_{M3}, λ_{S3}, and λ_{2SP} are determined according to (26), in which the quantities h_i are replaced by the characteristic linear space scales h_r, δ_1, and d, respectively, where $\delta_1 = (h_r + N_k^{-1})$ is the average height of the spherical gap between particles. It is important to note that in determining the thermal and electrical conductivities of an ultrafine system we have neglected the influence of thermoelectric inhomogeneity of the contact zone on λ and σ [22].

Comparison with Experimental Data

In real particulate systems several of the parameters have a definite scatter (height h_r of the microasperities, particle diameter d, areas of the nominal and actual contact spot,

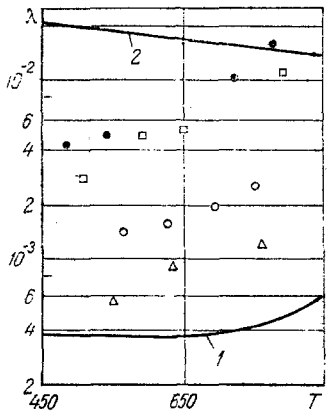

Fig. 3

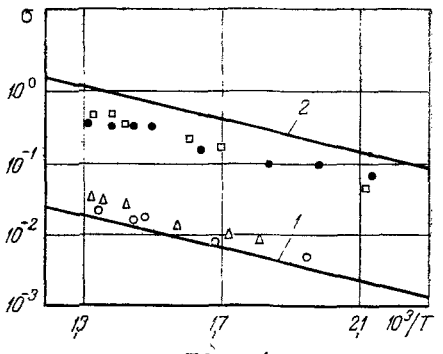

Fig. 4

Fig. 3. Thermal conductivity of ultrafine n-Ge. Calculated curves: 1) λ_{min}; 2) λ_{max}. Experimental points for four samples prepared under identical conditions [6]. λ, W/m•°K; T, °K.

Fig. 4. Electrical conductivity of ultrafine n-Ge. Calculated curves: 1) σ_{min}; 2) σ_{max}. Experimental points for four samples prepared under identical conditions [6]. σ, $\Omega^{-1}cm^{-1}$; T, °K.

etc.). As a result, for the thermal and electrical conductivities λ and σ we can only indicate an interval in which their values lie. For particulate systems at atmospheric and higher pressures this scatter is small for λ, because in this case the main heat flux is realized through the gaseous component. For particulate systems in vacuum the interval of possible values of λ and σ is larger.

Calculations of λ_m and σ_m according to (14) and (25) show that increasing y_{2e}/y_1 from 1 to 10^2 has the effect of increasing β_m/β_1 from 1 to 10^3. Consequently, to increase z in particulate systems a necessary condition is point contact, in which case $y_1 \ll y_2$.

The values of λ and σ calculated according to (14), (25), and (1) are compared with experimental data [6] on the thermal and electrical conductivities of ultrafine n-Ge in vacuum (H = 10^{-7} mm Hg) in Figs. 3 and 4. At T = 300°K the thermal and electrical conductivities of n-Ge have the following values: λ_1 = 60 W/m•°K; σ_1 = 16 $\Omega^{-1}cm^{-1}$. The average grain diameter is 2 to 2.5 μm.

In calculating the minimum effective thermal conductivity λ_{min} we determined y_2 from (8) and assumed y_1 to be equal to $y_1 = 10^{-2}y_2$; see (10). In calculating λ_{max} we assumed y_1 to be equal to $y_1 = 10^{-1}y_2$. In addition, $y_2 \approx 5 \cdot 10^{-2}$; h_r = 20 Å; ε = 0.5.

It is evident from Fig. 3 that the calculations give different temperature dependences for λ_{min} and λ_{max}. The thermal conductivity λ_{min} at T < 650°K remains constant, and at T ≥ 650°K it increases (see Fig. 3). The coefficient λ_{max} decreases with increasing temperature. This behavior is attributable to the fact that in calculating the effective thermal conductivity λ we considered the thermal conductivity λ_1 of the grains to be equal to the thermal conductivity of crystalline n-Ge, and the latter coefficient decreases with increasing temperature. For relatively large values of y_1, therefore, such that the main heat flux is realized through the contact spot, λ_{max} decreases as λ_1 decreases. For small values of y_1 at temperatures T > 500°K radiative heat transfer between grains begins to assert itself, causing λ_{min} to increase.

The minimum value σ_{min} and maximum value σ_{max} of the electrical conductivity were determined for the same values of y_2 and y_1 (see Fig. 4). The electrical conductivity across the contact gap, σ_2, was determined according to (17). In calculating σ_{min} we assumed the value of ν_2 to be equal to zero. An estimate of σ_2 has shown that over the entire temperature range range ν_2 may be considered to be constant and equal to $\nu_2 \approx 10^{-2}$; this was the value used in the calculation of σ_{max}.

Calculations according to (14), (25), and (1) show that for a constant ratio β/β_1 the values of λ and σ increase if the porosity of the system is decreased, without plastic deformation of the particles, from an initial value m_2^0 to $m_{2k}^0 = 0.4$. This effect can be achieved

by vibration shakedown of the particulate system. According to (14) and (25), an increase in β/β_1 will be observed with a decrease in the particle diameter, i.e., as $y_{2e} \to y_2$. This condition obtains for $d < 1$ μm ($h_r < 100$ Å).

It is essential to note that the lack of a good set of experimental data on superficially sintered ultrafine disperse systems prevents us from making an extensive comparison with the postulated analytical relations. However, an analysis of the existing data fosters the expectation that the proposed model and analytical relations will provide a first approximation in calculations and analysis of the influence of the energy barriers at the grain boundaries (contacts) on transfer processes in superficially sintered ultrafine systems.

NOTATION

α, thermoelectric emf; σ, electrical conductivity; λ, thermal conductivity; $\varkappa_m$, linear deformation of particles; N_m, coordination number; Λ, effective general conductivity of particulate system; r_2, radius of nominal contact spot; r_1, radius of actual contact spot; E_S, elastic modulus of particulate system; E_M, elastic modulus of particle material; P'_{sp}, specific external pressure; D, diffusion coefficient; K, Boltzmann constant; T, temperature; d, particle diameter; h_r, roughness (microasperity) height of particles; $\bar{h}_r = h_r/r$; h_e, height of contact gap when the current across the gap is commensurate with the current across the actual contact spot; $\varepsilon = h_e/h_r$; $r_{2e} = \varepsilon r_2$; C, Richardson constant; e, electron charge; $\bar{v}$, height of gap potential barrier; $\hbar = h/2\pi$, Planck constant; m*, effective mass of electron; ε_1, dielectric constant of particles; ε_2, dielectric constant of gap; E, electric field; V, voltage applied to sample; $h_{\mathcal{L}a}$, height of free-flowing particle layer; φ_0, work function; φ^*, image force potential; ε_{re}, reduced emissivity; σ_{S-B}, Stefan—Boltzmann constant; $\beta = \sigma/\lambda$; $\beta_1 = \sigma_1/\lambda_1$; $\nu_2 = \sigma_2/\sigma_1$.

LITERATURE CITED

1. A. F. Ioffe, Semiconductor Thermoelements [in Russian], Akad. Nauk SSSR, Moscow (1956).
2. A. F. Ioffe, Selected Works [in Russian], Vol. 2, Nauka, Leningrad (1975).
3. M. Green, U. S. Patent No. 3524771: Semiconductor Devices, Cl. 136-203 (1970).
4. B. M. Gol'tsman et al., Izv. Akad. Nauk SSSR, Neorg. Mater., 5, No. 2 (1969).
5. N. S. Lidorenko et al., Izv. Akad. Nauk SSSR, Neorg. Mater., 6, No. 12 (1969).
6. L. S. Stil'bans, A. D. Terekhov, and É. M. Sher, in: Proceedings of the All-Union Conference on Dimensional and Deformation Effects in Thermoelectric Materials and Films [in Russian], Leningrad (1976).
7. V. I. Odelevskii, Zh. Tekh. Fiz., 21, 678 (1951).
8. G. N. Dul'nev, Inzh.-Fiz. Zh., 9, 399 (1965).
9. L. L. Vasil'ev, in: Investigation of Thermal Conductivity [in Russian], Nauka i Tekhnika, Minsk (1967), p. 262.
10. G. N. Dul'nev and Yu. P. Zarichnyak, Thermal Conductivity of Mixtures and Heterogeneous Materials [in Russian], Énergiya, Leningrad (1974).
11. G. N. Dul'nev and V. V. Novikov, Inzh.-Fiz. Zh., 33, No. 2 (1977).
12. L. D. Landau and E. M. Lifshits, Theoretical Physics, Vol. 7: Theory of Elasticity [in Russian], Nauka, Moscow (1965).
13. Z. V. Sigalova, Candidate's Dissertation, Leningrad Institute of Precision Mechanics and Optics, Leningrad (1965).
14. Ya. E. Geguzin, Physics of Sintering [in Russian], Nauka, Moscow (1967).
15. L. L. Vasil'ev and S. A. Tanaeva, Thermophysical Properties of Porous Materials [in Russian], Nauka i Tekhnika, Minsk (1971).
16. V. I. Strikha, Theoretical Foundations of the Work of a Metal—Semiconductor Contact [in Russian], Naukova Dumka, Kiev (1974).
17. N. Mostovetch, Compt. Rend. Acad. Sci., 233, 360 (1951).
18. J. S. Simmons, J. Appl. Phys., 34, No. 6 (1963).
19. C. E. Drumheller, J. Phys. (Paris), 25, 198 (1964).
20. V. I. Glybin, Ukrainsk. Fiz. Zh., 16, No. 8 (1971).
21. H. A. Bethe and A. Sommerfeld, Electronic Theory of Metals [Russian translation], GITTL, Leningrad—Moscow (1938).
22. G. N. Dul'nev and V. V. Novikov, Inzh.-Fiz. Zh., 33, No. 3 (1977).